Progress In Electromagnetics Research M, Vol. 90, 109–116, 2020

Solving Electric Current Volume Integral Equation with Nonconformal Discretization and Sherman-Morrison-Woodbury Formula-Based Algorithm

Fei Huang[1, 2] and Yufa Sun[1, *]

Abstract—A fast direct solution of the electric current volume integral equation (JVIE) with the Sherman-Morrison-Woodbury (SMW) formula-based algorithm is presented to analyze electromagnetic scattering from inhomogeneous dielectric objects. The JVIE is discretized with the nonconformal face-based Schaubert-Wilton-Glisson (SWG) basis functions. Compared with conformal discretization that is advantageous to discrete homogeneous regions, the nonconformal discretization provides a more flexible and efficient scheme to separately handle the inhomogeneous subdomains depending on local parameters. Moreover, to take full use of both discretization methods, the mixture discretization is adopted. With the increase of object size, the impedance matrix equation arising from the JVIE becomes too large to solve and store for direct solution. In this paper, the SMW formula-based algorithm is adopted, leading to remarkable reduction on the computational complexity and memory requirement in contrast with conventional direct solution. This algorithm compresses the impedance matrix into a product of block diagonal submatrices, which can be inversed rapidly in direct way. Numerical results are given to demonstrate the efficiency and accuracy of the proposed method.

1. INTRODUCTION

Volume integral equation (VIE) method has been widely used to analyze electromagnetic scattering from inhomogeneous dielectric objects [1]. Usually the conformal discretization is adopted to convert VIE into a matrix equation for enforcing the normal continuity of electric currents across adjacent volume elements [2]. For objects with multiscale structure or high-contrast relative permittivity, the conformal discretization may result in barriers to analysis efficiency. It is mainly because the small geometric structures or high-contrast subdomains which are discretized with same mesh size as the remaining components may generate excessive elements [3]. Hence, it is essential to integrate the nonconformal discretization into VIE. Depending on local physical parameters, the subdomains are permitted to independently adopt individual mesh size or high-order basis function without restriction of continuity condition [4], which reduces the number of elements for modeling complex objects. In addition, the equivalent electric currents are used to expand the VIE in our study. Compared with the electric flux-based [5] or electric field-based [6] VIE, the electric current volume integral equation (JVIE) is independent on the material parameter in integral kernel, expediting the calculation of the impedance matrix [7].

In consideration of unpredictable convergence of iterative solver, the direct solver is employed to solve the matrix equation derived from the JVIE [8]. Furthermore, the direct solver exhibits significant advantage over the iterative solver on dealing with the problems with multiple right-hand-side vectors.

Received 17 December 2019, Accepted 5 March 2020, Scheduled 6 March 2020

* Corresponding author: Yufa Sun (yfsun_ahu@sina.com).

[1] Key Lab of Intelligent Computing & Signal Processing, Ministry of Education, Anhui University, Hefei 230601, China. [2] School of Mechanical and Electronics Engineering, Suzhou University, Suzhou, Anhui 234000, China.

For each new vector, the iterative solver needs to resume, leading to more computational consumption than the direct solver. However, scaled with $O(N^3)$ and $O(N^2)$, respectively, the computational complexity and memory requirement of direct solver are too expensive for large objects, where N denotes the number of the unknowns. Hence, the multiscale compressed block decomposition (MSCBD) [9] and Sherman-Morrison-Woodbury (SMW) formula-based algorithm (SMWA) [10, 11] are proposed to improve the efficiency. The two algorithms follow a similar key idea that decompose the impedance matrix into a hierarchical structure composed of the sparse approximation of submatrices, which are easy to inverse and store. Of the two algorithms, the SMWA is more suitable for parallelization.

Each of the conformal and nonconformal discretization has advantages and drawbacks. To make full use of their advantages, the mixture of both discretization methods is adopted to discrete the JVIE. Moreover, the SMWA is employed to solve the matrix equation. It decomposes the impedance matrix into the product of low-dimension matrices, which are sparse and easy to inverse. Then it approximates the inverse of the original matrix with the product of the inverse of the low-dimension sparse matrices. Compared with the conventional LU algorithm which solves the high-dimension matrix equation extremely slowly, the SMWA is more efficient, saving remarkable computational resources in terms of both CPU time and memory.

2. FORMULATION

2.1. The JVIE and Nonconformal Discretization

An arbitrarily shaped inhomogeneous object with the complex permittivity $\varepsilon(r)$ residing in the free space with the permittivity ε_0 and permeability μ_0 is excited by the incident electric field $\mathbf{E}^{\text{inc}}(r)$. According to the volume equivalence principle, the JVIE can be formulated as

$$\frac{\mathbf{J}(r)}{j\omega\varepsilon(r)\kappa(r)} + j\omega\mathbf{A}(r) + \nabla\Phi(r) = \mathbf{E}^{\text{inc}}(r) \tag{1}$$

where ω is the working angular frequency; $\mathbf{J}(r)$ represents the equivalent volume currents; and $\kappa(r) = 1 - \varepsilon_0/\varepsilon(r)$ denotes the contrast ratio. The vector potential $\mathbf{A}(r)$ and scalar potential $\Phi(r)$ are related to $\mathbf{J}(r)$. The vector potential $\mathbf{A}(r)$ can be written as

$$\mathbf{A}(r) = \mu_0 \int_V \mathbf{J}(r')G\left(r, r'\right) dv' \tag{2}$$

where $G(r, r') = \exp(-jk_0|r - r'|)/(4\pi|r - r'|)$ is Green's function with r being position vector of the observation point and r' being position vector of the source point, and k_0 is the wave number of free space. For JVIE, the equivalent volume currents $\mathbf{J}(r)$ are physically noncontinuous across the interface separating different mediums. Hence, the equivalent surface charges $\varphi_s(r)$ that only accumulate on the mediums interface are introduced to enforce the current continuity. Correspondingly, the scalar potential $\Phi(r)$ can be expressed in the form of the volume charges $\varphi_v(r)$ and surface charges $\varphi_s(r)$

$$\Phi(r) = \frac{1}{\varepsilon_0}\left[\int_V \varphi_v(r')G\left(r, r'\right) dv' + \int_{S_{\text{inter}}} \varphi_s(r')G\left(r, r'\right) ds'\right] \tag{3}$$

where S_{inter} represents a set of interfaces between different mediums in the object. $\varphi_v(r')$ and $\varphi_s(r')$ accord with the following equations, respectively

$$\varphi_v(r') = (j/\omega)\nabla' \cdot \mathbf{J}\left(r'\right) \tag{4}$$

$$\varphi_s(r') = (j/\omega)\sum_{m=1}^{M} n_{\text{inter}}^m \cdot \left[\mathbf{J}_p\left(r'\right) - \mathbf{J}_q\left(r'\right)\right] \tag{5}$$

where n_{inter}^m denotes the unit vector normal to the interface S_{inter}^m, of which the number is M. $\mathbf{J}_p(r')$ and $\mathbf{J}_q(r')$ respectively indicate the induced volume currents in two tetrahedrons which share the common face S_{inter}^m. For the reason that $\mathbf{J}_p(r')$ and $\mathbf{J}_q(r')$ are discontinuous, the conformal Schaubert–Wilton–Glisson (SWG) basis functions [12] are incapable to directly expand $\mathbf{J}_p(r')$ and $\mathbf{J}_q(r')$. Herein, the

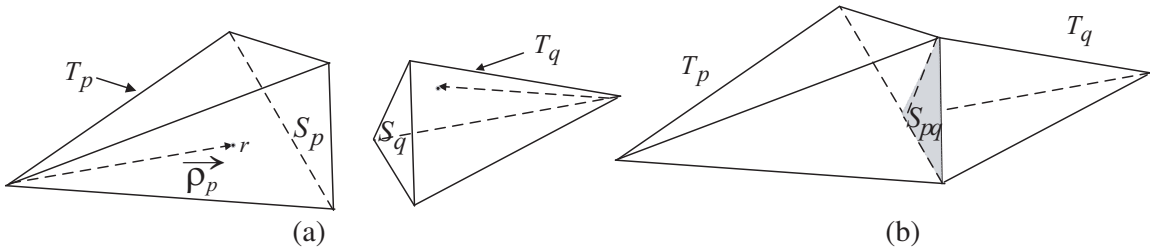

Figure 1. Nonconformal discretization with mono-SWG basis functions. (a) Definition of mono-SWG basis function. (b) Illumination of nonconformal discretization.

nonconformal SWG basis function $f_p(r)$, termed as mono-SWG basis function, is introduced to address the problem.

As presented in Fig. 1(a), $f_p(r)$ associated with face S_p is defined within single tetrahedron T_p

$$f_p(r) = \begin{cases} \dfrac{a_p}{3V_p}\rho_p, & r \in T_p \\ 0, & \text{otherwise} \end{cases} \tag{6}$$

where a_p and V_p are the area of face S_p and the volume of tetrahedron T_p, respectively, and ρ_p denotes the vector with respect to the vertex opposite to face S_p. The electric current within each single tetrahedron can be represented by the sum of four linearly independent mono-SWGs (one associated with each face). The electric currents in T_p and T_q can be expressed respectively as

$$\mathbf{J}_p(\mathbf{r}) = \sum_{k=1}^{4} \beta_{pk} f_{pk}(r) \tag{7}$$

$$\mathbf{J}_q(\mathbf{r}) = \sum_{k=1}^{4} \beta_{qk} f_{qk}(r) \tag{8}$$

where β_{pk} and β_{qk} represent the expanded coefficients of the corresponding mono-SWG basis functions. Substituting Eqs. (7) and (8) into Eq. (5), because only the basis function $f_{pm}(r)$ and $f_{qm}(r)$ whose corresponding face is S^m_{inter} has component normal to S^m_{inter}, $\varphi_s(r')$ can be simplified as

$$\varphi_s(r') = (j/\omega) \sum_{m=1}^{M} (\beta_{pm} - \beta_{qm}) \tag{9}$$

where β_{pm} and β_{qm} indicate the coefficients of two mono-SWG basis functions, which are associated with the interface S^m_{inter}.

The integral kernel of the vector potential $\mathbf{A}(r)$ and the scalar potential $\Phi(r)$ for the electric flux-based and electric field-based VIE depend on the material parameter $\kappa(r)$. However, it can be seen from aforementioned equations that both $\mathbf{A}(r)$ and $\Phi(r)$ for JVIE are unrelated with $\kappa(r)$ or $\varepsilon(r)$, which will accelerate the calculation of impedance matrix elements.

The illumination of nonconformal discretization, which uses two mono-SWG basis functions defined in adjacent tetrahedrons with different mesh sizes T_p and T_q, is presented in Fig. 1(b). The surface charges accumulating on the shadow area S_{pq} enforce the current continuity across adjacent tetrahedrons. Integrating the nonconformal discretization into JVIE can impose current continuity on the mediums interface and handle extremely multiscale targets with flexible discretization scheme, significantly reducing the number of volume elements required for modeling.

2.2. The SMWA

In the following, the SMWA as a recursive algorithm is introduced to inverse the impedance matrix derived from the JIVE. It firstly implements the multilevel binary tree division on the geometry of the object to transform the impedance matrix into a hierarchical structure. At level 1, the object is

divided into two blocks. As a result, the impedance matrix $\mathbf{Z}$ is partitioned into four submatrices, of which the off-diagonal submatrices with low-rank property can be compressed by the adaptive cross approximation (ACA) algorithm. Matrix $\mathbf{M}$ is the sparse approximation of $\mathbf{Z}$

$$\mathbf{Z} \approx \mathbf{M} = \begin{bmatrix} \mathbf{M}_{11}^1 & \mathbf{U}_{12}^1(\mathbf{V}_{12}^1)^T \\ \mathbf{U}_{21}^1(\mathbf{V}_{21}^1)^T & \mathbf{M}_{22}^1 \end{bmatrix} \tag{10}$$

where $\mathbf{M}_{11}^1$ and $\mathbf{M}_{22}^1$ denote the self-impedance matrix of two blocks at level 1, respectively, $\mathbf{U}_{12}^1$, $\mathbf{V}_{12}^1$, $\mathbf{U}_{21}^1$, and $\mathbf{V}_{21}^1$ indicate the ACA decomposition matrices. Then $\mathbf{M}$ is written as

$$\begin{aligned} \mathbf{M} &= \begin{bmatrix} \mathbf{M}_{11}^1 & \mathbf{0} \\ \mathbf{0} & \mathbf{M}_{22}^1 \end{bmatrix} \begin{bmatrix} \mathbf{I} & (\mathbf{M}_{11}^1)^{-1}\mathbf{U}_{12}^1(\mathbf{V}_{12}^1)^T \\ (\mathbf{M}_{22}^1)^{-1}\mathbf{U}_{21}^1(\mathbf{V}_{21}^1)^T & \mathbf{I} \end{bmatrix} \\ &= \mathbf{M}_R^1\mathbf{M}^1 \end{aligned} \tag{11}$$

where $\mathbf{M}_R^1$ is a block diagonal matrix composed of the self-impedance submatrices at level 1, and $\mathbf{M}^1$ comprises identity matrix $\mathbf{I}$ and product of low-rank matrices. $\mathbf{M}_R^1$ can be factorized by progressively partitioning $\mathbf{M}_{11}^1$ and $\mathbf{M}_{22}^1$ and recursively calling the SMWA until the finest level. Fig. 2 presents the illustration of 3-level factorization of the impedance matrix $\mathbf{M}$.

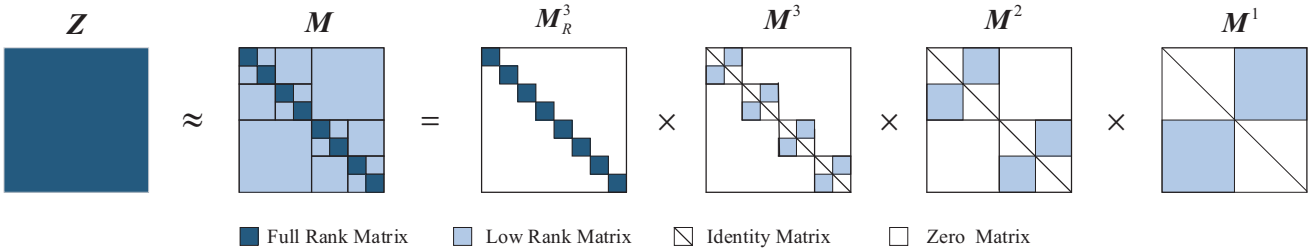

Figure 2. The illustration of 3-level factorization of the impedance matrix $\mathbf{Z}$.

At level L, $\mathbf{M}$ is decomposed into a product of $L+1$ block diagonal matrices

$$\mathbf{M} = \mathbf{M}_R^L\mathbf{M}^L\mathbf{M}^{L-1}\dots\mathbf{M}^1 \tag{12}$$

Then the inverse of $\mathbf{M}$ can be calculated by

$$\mathbf{M}^{-1} = (\mathbf{M}^1)^{-1}\dots(\mathbf{M}^{L-1})^{-1}(\mathbf{M}^L)^{-1}(\mathbf{M}_R^L)^{-1} \tag{13}$$

where $\mathbf{M}_R^L$ consists of 2^L diagonal submatrices with size of $(N/2^L)\times(N/2^L)$, which can be easily inversed. N is the number of unknowns in $\mathbf{Z}$. For $\mathbf{M}^l$ $(1 \le l \le L)$, these matrices are similar in form of identity matrices and product of low-rank matrices. With the aid of the SMW formula $(\mathbf{I}+\mathbf{AB})^{-1} = \mathbf{I}-\mathbf{A}(\mathbf{I}+\mathbf{BA})^{-1}\mathbf{B}$, it is efficient to inverse $\mathbf{M}^l$. Taking $\mathbf{M}^1$ for instance, $\mathbf{M}^1$ is firstly adapted as

$$\mathbf{M}^1 = \begin{bmatrix} \mathbf{I} & \mathbf{0} \\ \mathbf{0} & \mathbf{I} \end{bmatrix} + \mathbf{A}_Z\mathbf{B}_Z \tag{14}$$

$$\mathbf{A}_Z = \begin{bmatrix} \mathbf{0} & (\mathbf{M}_{11}^1)^{-1}\mathbf{U}_{12}^1 \\ (\mathbf{M}_{22}^1)^{-1}\mathbf{U}_{21}^1 & \mathbf{0} \end{bmatrix} \tag{15}$$

$$\mathbf{B}_Z = \begin{bmatrix} (\mathbf{V}_{21}^1)^T & \mathbf{0} \\ \mathbf{0} & (\mathbf{V}_{12}^1)^T \end{bmatrix} \tag{16}$$

then $(\mathbf{M}^1)^{-1}$ can be calculated by

$$(\mathbf{M}^1)^{-1} = \mathbf{I}-\mathbf{A}_Z(\mathbf{I}+\mathbf{B}_Z\mathbf{A}_Z)^{-1}\mathbf{B}_Z \tag{17}$$

where matrix $\mathbf{I}+\mathbf{B}_Z\mathbf{A}_Z$ is much smaller than $\mathbf{M}^1$. Following aforementioned rules, we can calculate the inverse of $\mathbf{M}^l$ with greatly less computational and memory consumption, and $\mathbf{Z}^{-1} \approx \mathbf{M}^{-1}$ can be rapidly obtained. To be clearer, the pseudo code of the SMWA is presented in Fig. 3.

Function $\boldsymbol{M}^{-1} = \text{SMWA}(\boldsymbol{M})$
  if $\boldsymbol{M}$ is the impedance matrix of the finest sub-block
    inverse $\boldsymbol{M}$ by LU decomposition then return $\boldsymbol{M}^{-1}$
  else
    partition the $\boldsymbol{M}$ into $\boldsymbol{M}_{11}$, $\boldsymbol{M}_{22}$, $\boldsymbol{M}_{12}$ and $\boldsymbol{M}_{21}$
    $[\boldsymbol{U}_{12}, \boldsymbol{V}_{12}^T] = \text{ACA}(\boldsymbol{M}_{12})$
    $[\boldsymbol{U}_{21}, \boldsymbol{V}_{21}^T] = \text{ACA}(\boldsymbol{M}_{21})$
    $\boldsymbol{M}_{11}^{-1} = \text{SMWA}(\boldsymbol{M}_{11})$
    $\boldsymbol{M}_{22}^{-1} = \text{SMWA}(\boldsymbol{M}_{22})$
    Inverse $\begin{bmatrix} \boldsymbol{I} & \boldsymbol{M}_{11}^{-1}\boldsymbol{U}_{12}\boldsymbol{V}_{12}^T \\ \boldsymbol{M}_{22}^{-1}\boldsymbol{U}_{21}\boldsymbol{V}_{21}^T & \boldsymbol{I} \end{bmatrix}$ by SMW formula
    Return $\begin{bmatrix} \boldsymbol{I} & \boldsymbol{M}_{11}^{-1}\boldsymbol{U}_{12}\boldsymbol{V}_{12}^T \\ \boldsymbol{M}_{22}^{-1}\boldsymbol{U}_{21}\boldsymbol{V}_{21}^T & \boldsymbol{I} \end{bmatrix}^{-1} \begin{bmatrix} \boldsymbol{M}_{11}^{-1} & 0 \\ 0 & \boldsymbol{M}_{22}^{-1} \end{bmatrix}$

Figure 3. The pseudo code of the SMWA.

2.3. The Mixture of Conformal and Nonconformal Discretization

For piecewise homogeneous dielectric object, the normal component of $\mathbf{J}(r)$ is continuous in the homogeneous part of the object, where using the conformal SWG basis functions to expand $\mathbf{J}(r)$ is more efficient. It is for the reason that in homogeneous area the conformal discretization generates less unknowns. To improve the efficiency of the algorithm, we mix the conformal and nonconformal discretization to discrete the JVIE. As presented in Fig. 4, the mono-SWG basis functions are applied to model the boundaries separating two mediums, meanwhile, the conformal SWG basis functions are used to model the inner of homogenous parts.

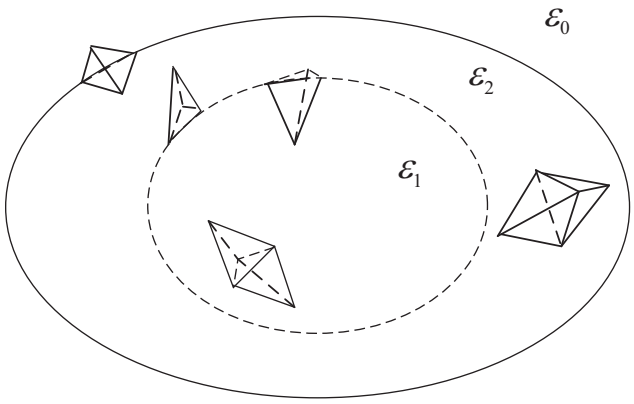

Figure 4. Two discretization methods for dielectric object with two homogeneous subdomains.

3. NUMERICAL RESULTS

To validate the accuracy and efficiency of proposed hybrid of nonconformal discretization and SMWA on solving JVIE, the monostatic radar cross section (RCS) of inhomogeneous dielectric object is calculated for vertical polarization (VV) with incident plane waves at 300 MHz. The plane waves for calculating the monostatic RCS are normally θ-polarized and set in the range from $\theta = 0^\circ$ to $\theta = 180^\circ$ ($\phi = 0^\circ$).

In order to estimate the error of the proposed method, the root mean square (RMS) error of the RCS is introduced, which is defined as

$$\mathrm{RMS\,(dB\,sm)} = \sqrt{\frac{1}{N_2}\sum_{i=1}^{N_a}\left|\sigma_{ref,i} - \sigma_{pro,i}\right|^2} \tag{18}$$

where $\sigma_{pro,i}$ denotes the RCS calculated by the proposed method, and $\sigma_{ref,i}$ stands for the reference result, N_a is the number of the sampling angles.

The first example is a composite inhomogeneous object, which is composed of a cube with size of 0.5 m × 0.5 m × 0.2 m and a cylinder with radius of 0.1 m and height of 0.05 m. The cylinder is placed on the center of the cube top surface, as shown in Fig. 5. The relative permittivities of the cube and cylinder are $\varepsilon_{cu} = 4.0$ and $\varepsilon_{cy} = 16.0$, respectively. For modeling the composite object, the numbers of tetrahedrons and unknowns produced by the conformal, nonconformal and mixture discretization are compared in Table 1. It is shown that the mixture discretization produces the least unknowns, gaining the most efficiency. The nonconformal electric flux-based VIE (NDVIE) that applies the LU algorithm to solve the matrix equation is taken as reference method [13]. The monostatic RCSs of composite object calculated by NDVIE and the proposed method that applies the SMWA to solve the matrix equation are depicted in Fig. 5. It is shown that the two results fit well. The RMS between two methods is 0.08 dBsm. The CPU time and memory of the NDVIE and proposed method for calculating RCS are presented in Table 2. Compared with the NDVIE, the proposed method saves about 62.8% and 52.2% in terms of total CPU time and memory requirement, respectively.

The pyramid-shaped object with base square length of 0.6 m and height of 0.9 m is evenly divided into three layers along the z-axis as shown in Fig. 6. The relative permittivities of the top, middle, and bottom layer are $\varepsilon_1 = 16.0$, $\varepsilon_2 = 4.0$, and $\varepsilon_3 = 9.0$, respectively. For modeling the pyramid-

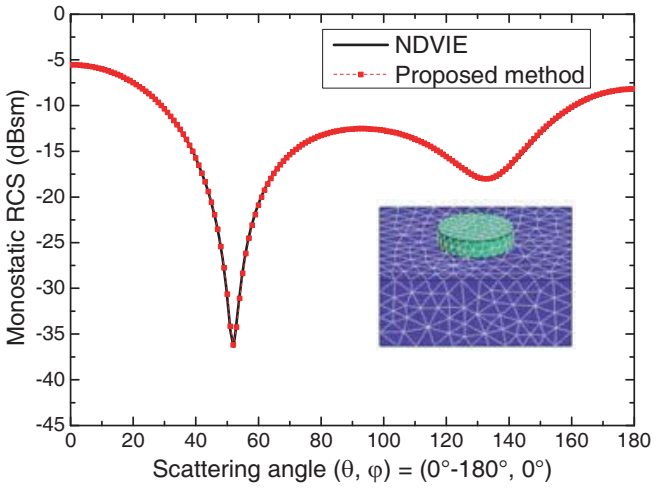

Figure 5. Monostatic RCS of composite object for VV polarization.

Table 1. The number of tetrahedrons and unknowns for modeling by three discretization methods.

Discretization method	Composite object		Pyramid-shaped object	
	Number of tetrahedrons	Number of unknowns	Number of tetrahedrons	Number of unknowns
Conformal	32363	66943	65765	128370
Nonconformal	4654	18616	25695	102780
Mixture	4654	9775	25695	53431

Table 2. The CPU time and memory of the NDVIE and proposed method for calculating the RCS.

Object	NDVIE		Proposed method	
	Time (s)	Memory (MB)	Time (s)	Memory (MB)
Composite object	849	764	315	365
Pyramid-shaped object	37268	22838	5016	4926

shaped object, the numbers of tetrahedrons and unknowns produced by the conformal, nonconformal and mixture discretization are compared in Table 1, where the mixture discretization generates the least unknowns. The monostatic RCSs of pyramid-shaped object calculated by NDVIE and the proposed method are depicted in Fig. 6, where two results agree well with each other. The RMS between two methods is 0.11 dBsm. The computational consumptions of the NDVIE and proposed method are presented in Table 2. In comparison to NDVIE, the proposed method saves about 86.5% and 78.4% in terms of total CPU time and memory requirement, respectively.

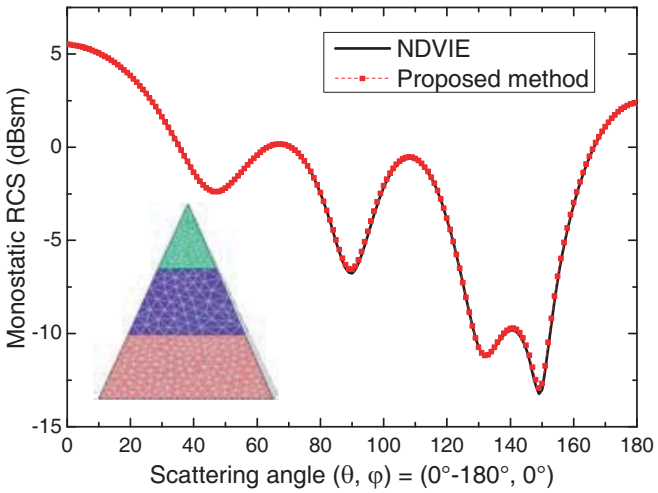

Figure 6. Monostatic RCS of pyramid-shaped object for VV polarization.

4. CONCLUSION

In this paper, the mixture of conformal and nonconformal discretization has been used to convert the JVIE, greatly reducing the number of elements and unknowns for modeling. Furthermore, by means of SMWA, the generated matrix equation is solved with remarkably less computational and memory consumption. The accuracy and efficiency have been validated by two inhomogeneous objects.

ACKNOWLEDGMENT

This work was supported by the National Natural Science Foundation of China (grant 61172020) and Project of Anhui Local High-level University Construction (grant 2013gx001). It was also supported by the Scientific Research Platform Project of Suzhou University under Grant 2016ykf01.

REFERENCES

1. Schaubert, D. H. and P. M. Meaney, "Efficient computation of scattering by inhomogeneous dielectric bodies," *IEEE Trans. Antennas Propagat.*, Vol. 34, No. 4, 587–592, 1986.

2. Peng, Z., K.-H. Lee, and J.-F. Lee, "A discontinuous Galerkin surface integral equation method for electromagnetic wave scattering from nonpenetrable targets," *IEEE Trans. Antennas Propag.*, Vol. 61, No. 7, 3617–3628, 2013.
3. Cai, Q.-M., et al., "Nonconformal discretization of electric current volume integral equation with higher order hierarchical vector basis functions," *IEEE Trans. Antennas Propag.*, Vol. 65, No. 8, 4155–4169, 2017.
4. Nair, N. and B. Shanker, "Generalized method of moments: A novel discretization technique for integral equation," *IEEE Trans. Antennas Propag.*, Vol. 59, No. 6, 2280–2293, 2011.
5. Botha, M. M., "Solving the volume integral equations of electromagnetic scattering," *J. Comput. Phys.*, Vol. 218, No. 1, 141–158, 2006.
6. Markkanen, J., C.-C. Lu, X. Cao, and P. Ylä-oijala, "Analysis of volume integral equation formulations for scattering by high-contrast penetrable objects," *IEEE Trans. Antennas Propag.*, Vol. 60, No. 5, 2367–2374, 2012.
7. Zhang, L.-M. and X.-Q. Sheng, "A discontinuous Galerkin volume integral equation method for scattering from inhomogeneous objects," *IEEE Trans. Antennas Propag.*, Vol. 63, No. 12, 5661–5667, 2015.
8. Heldring, A., J. M. Rius, J. M. Tamayo, J. Parrón, and E. úbeda, "Fast direct solution of method of moments linear system," *IEEE Trans. Antennas Propag.*, Vol. 55, No. 2, 3220–3228, 2007.
9. Heldring, A., J. M. Rius, J. M. Tamayo, J. Parrón, and E. Ubeda, "Multiscale compressed block decomposition for fast direct solution of method of moments linear system," *IEEE Trans. Antennas Propag.*, Vol. 59, No. 2, 526–536, 2011.
10. Chen, X.-L., C.-Q. Gu, Z. Li, and Z. Niu, "Accelerated direct solution of electromagnetic scattering via characteristic basis function method with Sherman-Morrison-Woodbury formula-based algorithm," *IEEE Trans. Antennas Propag.*, Vol. 64, No. 10, 4482–4486, 2016.
11. Fang, X.-X., Q.-S. Cao, Y. Zhou, and Y. Wang, "Multiscale compressed and spliced Sherman-Morrison-Woodbury algorithm with characteristic basis function method," *IEEE Trans. Electromagn. Compat.*, Vol. 60, No. 3, 716–724, 2018.
12. Schaubert, D. H., D. R. Wilton, and A. W. Glisson, "A tetrahedral modeling method for electromagnetic scattering by arbitrarily shaped inhomogeneous dielectric bodies," *IEEE Trans. Antennas Propag.*, Vol. 32, No. 1, 77–85, 1984.
13. Zhang, L.-M. and X.-Q. Sheng, "Discontinuous Galerkin volume integral equation solution of scattering from inhomogeneous dielectric objects by using the SWG basis function," *IEEE Trans. Antennas Propag.*, Vol. 65, No. 3, 1500–1504, 2017.